SCIENCE CHINA
Information Sciences

• **Supplementary File** •

A hybrid stochastic control strategy by two-layer networks for dissipating urban traffic congestion

Xiaojing ZHONG[1], Bin PANG[1], Feiqi DENG[2] & Xueyan ZHAO[2*]

[1]*School of Mechanical and Electrical Engineering, Guangzhou University, Guangzhou* 510006*, China;*
[2]*School of Automation Science and Engineering, South China University of Technology, Guangzhou* 510640*, China*

Appendix A Proof of Theorem 1

In model (1), Lipschitz property associated with the drift and diffusion coefficients implies the existence of a unique local solution on $[0, \omega_e]$, where ω_e is the explosion time [1]. Then, by using a proof by contradiction combined with a C^2 function to demonstrate that the explosion time tends to infinity, it proves the global uniqueness of the positvie solution in model (1). In fact, Theorem 3.1 in reference [2] and Theorem 2.1 in reference [3] both provide similar proofs, so we omit the specific proof steps.

Appendix B Proof of Theorem 2

To establish the validity of Theorem 2, we introduce the following lemmas and definition.

Lemma 1 (Exponential Martingale Inequality [1])**.** Let $g = (g_1, \cdots, g_m) \in \mathcal{L}^2(R_+; R^{1\times m})$, and let T, α, β be any positive numbers. Then

$$P\left\{\sup_{0\leqslant t\leqslant T}\left[\int_0^t g(s)\mathrm{d}B(s) - \frac{\alpha}{2}\int_0^t |g(s)|^2\,\mathrm{d}s\right] > \beta\right\} \leqslant e^{-\alpha\beta}.$$

Lemma 2. If the system parameters in the information layer satisfy $\Lambda_1\delta > \mu_1(\theta+\mu_1)$, we can get

$$\lim_{t\to\infty} S(t) = \frac{\Lambda_1\delta - \mu_1(\theta+\mu_1)}{(\theta+\mu_1)\delta} > 0,$$

which means congestion information will be effectively propagate.

Proof. From equilibrium equations on the information layer:

$$\begin{cases} \Lambda_1 - \delta I(t)S(t) - \mu_1 I(t) = 0 \\ \delta I(t)S(t) - \theta S(t) - \mu_1 S(t) = 0 \\ \theta S(t) - \mu_1 T(t) = 0, \end{cases} \tag{B1}$$

solving the above system of equations, we can see the information-free equilibrium $E_0 = (\frac{\Lambda_1}{\mu_1}, 0, 0)$ always exists, the endemic equilibrium $E_1 = (I_1^*, S_1^*, T_1^*)$ exists if and only if $\Lambda_1\delta > \mu_1(\theta+\mu_1)$, where

$$\begin{aligned} I_1^* =& \frac{\theta+\mu_1}{\delta}, \\ S_1^* =& \frac{\Lambda_1\delta - \mu_1(\theta+\mu_1)}{(\theta+\mu_1)\,\delta}, \\ T_1^* =& \frac{\Lambda_1\delta\theta - \Lambda_1\mu_1(\theta+\mu_1)}{(\theta+\mu_1)\delta\mu_1}. \end{aligned}$$

Then we prove the global stability of the endemic equilibrium E_1 under this condition.

Define a Lyapunov function

$$V_1(I, S) = I - I_1^* - I_1^*\log\frac{I}{I_1^*} + S - S_1^* - S_1^*\log\frac{S}{S_1^*},$$

Differentiating V_1 gives

$$\dot{V}_1 = \left(1 - \frac{I_1^*}{I}\right)(\Lambda_1 - \delta IS - \mu_1 I) + \left(1 - \frac{S_1^*}{S}\right)(\delta IS - \theta S - \mu_1 S)$$

We note that E_1 satisfy the following equations:

$$\begin{aligned} &\Lambda_1 - \delta I_1^* S_1^* - \mu_1 I_1^* = 0, \\ &\delta I_1^* S_1^* - \theta S_1^* - \mu_1 S_1^* = 0. \end{aligned}$$

* Corresponding author (email: auxyzhao@scut.edu.cn)

So we obtain

$$\begin{aligned}
\dot{V_1} &= \left(1-\frac{I_1^*}{I}\right)\left(\delta I_1^* S_1^* + \mu_1 I_1^* - \delta IS - \mu_1 I\right) + \left(1-\frac{S_1^*}{S}\right)\left(\delta IS - \delta I_1^* S\right)\\
&= -\frac{\mu_1}{I}\left(I-I_1^*\right)^2 + \delta\left(1-\frac{I_1^*}{I}\right)\left(I_1^* S_1^* - IS\right) + \delta S\left(1-\frac{S_1^*}{S}\right)\left(I-I_1^*\right)\\
&= -\frac{\mu_1}{I}\left(I-I_1^*\right)^2 + \delta\left(I_1^* S_1^* - IS - \frac{{I_1^*}^2 S_1^*}{I} + I_1^* S + IS - SI_1^* - S_1^* I + I_1^* S_1^*\right)\\
&= -\frac{\mu_1}{I}\left(I-I_1^*\right)^2 + \delta I_1^* S_1^*\left(2 - \frac{I_1^*}{I} - \frac{I}{I_1^*}\right)\\
&\leqslant 0,
\end{aligned}$$

which implies that $\dot{V_1} \leqslant 0$ for all $S, I > 0$. To show the global stability behavior of E_1, we investigate the largest compact invariant set where $\dot{V_1} = 0$. Observing the structure of $\dot{V_1}$, it is not difficult to notice that $\dot{V_1} = 0$ only at E_1. Therefore, by the LaSalle Invariant Principe [2], the endemic equilibrium E_1 is globally asymptotically stable. Namely,

$$\lim_{t\to\infty} S(t) = S_1^* = \frac{\Lambda_1\delta - \mu_1(\theta+\mu_1)}{(\theta+\mu_1)\delta} > 0,$$

congestion information will be effectively propagate.

The objective of this paper is to examine the almost sure exponential stability of model (1). We shall introduce the following definition for clarity.

Definition 1. Almost Sure Exponentially Stable [1]. The trivial solution of model (1) is said to be almost surely exponentially stable if

$$\limsup_{x\to\infty} \frac{1}{t}\log|x(t;t_0,x_0)| < 0 \quad a.s.$$

for all $x_0 \in R^d$.

Now, let's proceed to demonstrate Theorem 2.

For the social network layer, we first analyze the feasible domain of nodes, and the sum of the first three equations in model (1) yields,

$$\mathrm{d}[F(t)+C(t)+R(t)] = [\Lambda_2 - \mu_2(F(t)+C(t)+R(t))]\,\mathrm{d}t - \sigma_1[F(t)+C(t)+R(t)]\mathrm{d}B_1(t). \tag{B2}$$

The integral form can be written as

$$\begin{aligned}
F(t)+C(t)+R(t) = F(0)+C(0)+R(0)+\Lambda_2 t - \mu_2\int_0^t [F(s)+C(s)+R(s)]\mathrm{d}s\\
-\sigma_1\int_0^t [F(s)+C(s)+R(s)]\mathrm{d}B_1(s).
\end{aligned} \tag{B3}$$

By Lemma 4.2, Lemma 4.3 and setting $\mathrm{d}_S = \mathrm{d}_I = \mathrm{d}_R$, $\sigma_{1j} = \sigma_{2j} = \sigma_{3j} (1 \leqslant j \leqslant N)$ in Eq. (1.3) [2], we obtain

$$\lim_{t\to\infty}\frac{1}{t}\int_0^t \left(F(s)+C(s)+R(s)\right)\mathrm{d}B_1(s) = 0,$$

$$\lim_{t\to\infty}\frac{F(t)+C(t)+R(t)}{t} = 0.$$

Dividing both sides of Eq. (B3) by t and letting $t\to\infty$ yields,

$$\lim_{t\to\infty}\frac{1}{t}\int_0^t [F(s)+C(s)+R(s)]\mathrm{d}s = \frac{\Lambda_2}{\mu_2}. \tag{B4}$$

Next we begin to analyze whether $C(t)$ can be effectively controlled, that is, whether $C(t)$ tends zero almost surely. Applying $It\hat{o}'s$ formula to $C(t)$ we get

$$\mathrm{d}\log C(t) = \left[\alpha F(t) - r - \xi S(t) - \mu_2 - \frac{{\sigma_1}^2}{2} - \frac{{\sigma_2}^2 F^2(t)}{2}\right]\mathrm{d}t - \sigma_1\mathrm{d}B_1(t) + \sigma_2 F(t)\mathrm{d}B_2(t). \tag{B5}$$

Integrating both side of Eq. (B5) gives

$$\log C(t) = \log C(0) + \int_0^t \left[\alpha F(s) - \xi S(s) - \frac{1}{2}{\sigma_2}^2 F^2(s)\right]\mathrm{d}s - \left(\gamma + \mu_2 + \frac{{\sigma_1}^2}{2}\right)t - \sigma_1 B_1(t) + M(t). \tag{B6}$$

where $M(t) = \int_0^t \sigma_2 F(s)\mathrm{d}B_2(s)$ is a continuous martingales with $M(0) = 0$. Moreover, $\langle M(t), M(t)\rangle = \int_0^t {\sigma_2}^2 F^2(s)\mathrm{d}s$. For all $\forall\varepsilon\in(0,1)$, and letting $N = 0,1,2,\cdots$, by the exponential martingale inequality (Lemma 1)

$$P\left\{\sup_{0\leqslant t\leqslant (N+1)T}\left[M(t) - \frac{\varepsilon}{2}\langle M(t), M(t)\rangle\right] > \frac{2}{\varepsilon}\log(N+1)\right\} \leqslant \frac{1}{(N+1)^2}.$$

Utilizing the first part (a) of Borel-Cantelli's lemma, it follows that for almost all $\omega \in \Omega$, there exists an integer $N_0 = N_0(\omega)$ such that if $N > N_0$,

$$M(t) \leqslant \frac{\varepsilon}{2} \langle M(t), M(t) \rangle + \frac{2}{\varepsilon} log(N+1) \leqslant \frac{\varepsilon}{2} \int_0^t {\sigma_2}^2 F^2(s) \mathrm{d}s + \frac{2}{\varepsilon} log(N+1),$$

holds for all $0 \leqslant t \leqslant (N+1)T$. So Eq. (B6) goes to

$$\begin{aligned} \log C(t) = & \log C(0) - \xi \int_0^t S(s) \mathrm{d}s + \int_0^t \left[\alpha F(s) - \frac{(1-\varepsilon){\sigma_2}^2}{2} F^2(s) \right] \mathrm{d}s \\ & - \left(\gamma + \mu_2 + \frac{{\sigma_1}^2}{2} \right) t - \sigma_1 \mathrm{B}_1(t) + \frac{2}{\varepsilon} log(N+1), \end{aligned}$$

for all $t \leqslant (N+1)T$, $N \leqslant N_0$ almost surely. Consequently, for almost all $\omega \in \Omega$, if $NT \leqslant t \leqslant (N+1)T$ and $N \geqslant N_0$,

$$\begin{aligned} \frac{1}{t} \log C(t) = & \frac{\log C(0) + \frac{2}{\varepsilon} \log(N+1)}{N} + \sigma_1 \frac{B_1(t)}{t} - \frac{1}{t} \xi \int_0^t S(s) \mathrm{d}s \\ & + \frac{1}{t} \int_0^t \left[\alpha F(s) - \frac{(1-\varepsilon){\sigma_2}^2}{2} F^2(s) \right] \mathrm{d}s - \left(\gamma + \mu_2 + \frac{{\sigma_1}^2}{2} \right). \end{aligned} \tag{B7}$$

Note that $\lim_{t \to \infty} \frac{B_1(t)}{t} = 0$ *a.s.* by strong Law of large numbers. By the $L'H\hat{o}pital's$ Rule and Lemma 2, $\lim_{t\to\infty} \frac{1}{t} \int_o^t S(s) \mathrm{d}s = \lim_{t\to\infty} S(t) = S_1^*$. By the positivity of $S(t)$, $\lim_{t\to\infty} \frac{1}{t} \int_0^t S(s) \mathrm{d}s \geqslant 0$. Based on the comprehensive analysis above,

$$\lim_{t\to\infty} \frac{1}{t} \int_0^t S(s) \mathrm{d}s \geqslant \max\{0, S_1^*\}. \tag{B8}$$

Addittionally, the positivity of $C(t)$ and $R(t)$, along with the condition Eq. (B4), can be devived,

$$\lim_{t\to\infty} \frac{1}{t} \int_0^t F(s) \mathrm{d}s \leqslant \lim_{t\to\infty} \frac{1}{t} \int_0^t \left[F(s) + C(s) + R(s) \right] \mathrm{d}s = \frac{\Lambda_2}{\mu_2}.$$

Then we obtain,

$$\lim_{t\to\infty} \frac{1}{t} \int_0^t \left[\alpha F(s) - \frac{(1-\varepsilon){\sigma_2}^2}{2} F^2(s) \right] \mathrm{d}s \leqslant \min \left\{ \frac{\alpha \Lambda_2}{\mu_2}, \frac{\alpha^2}{2(1-\varepsilon){\sigma_2}^2} \right\}. \tag{B9}$$

With Eqs. (B8) and (B9), Eq. (B7) goes to

$$\limsup_{t\to\infty} \frac{1}{t} \log C(t) \leqslant - \max\{0, \xi S_1^*\} - \gamma - \mu_2 - \frac{{\sigma_1}^2}{2} + \min \left\{ \frac{\alpha \Lambda_2}{\mu_2}, \frac{\alpha^2}{2(1-\varepsilon){\sigma_2}^2} \right\} \quad a.s.$$

Let $\varepsilon \to 0$, we obtain,

$$\limsup_{t\to\infty} \frac{1}{t} \log C(t) \leqslant \min \left\{ \frac{\alpha \Lambda_2}{\mu_2}, \frac{\alpha^2}{2{\sigma_2}^2} \right\} - \max \left\{ 0, \frac{\xi[\Lambda_1 \delta - \mu_1(\theta + \mu_1)]}{(\theta + \mu_1)\delta} \right\} - \gamma - \mu_2 - \frac{{\sigma_1}^2}{2} \quad a.s.$$

If $\min \left\{ \frac{\alpha\Lambda_2}{\mu_2}, \frac{\alpha^2}{2{\sigma_2}^2} \right\} < \max \left\{ 0, \frac{\xi[\Lambda_1\delta - \mu_1(\theta+\mu_1)]}{(\theta+\mu_1)\delta} \right\} + \gamma + \mu_2 + \frac{1}{2}{\sigma_1}^2$, then $\limsup_{t\to\infty} \frac{1}{t} \log C(t) < 0$ *a.s.* The proof is complete.

Appendix C Proof of Corollaries

Corollary 1. For the model (1), if the condition ${\sigma_1}^2 > \frac{2\alpha\Lambda_2}{\mu_2} - 2\gamma - 2\mu_2$ is satisfied, then for any initial values, it holds that $\limsup_{t\to\infty} \frac{1}{t} \log C(t) < 0$ *a.s.*

Proof. The condition in Theorem 2 can be rewritten as

$$\min \left\{ \frac{\alpha \Lambda_2}{\mu_2(\gamma + \mu_2 + \frac{{\sigma_1}^2}{2})}, \frac{\alpha^2}{2{\sigma_2}^2(\gamma + \mu_2 + \frac{{\sigma_1}^2}{2})} \right\} - \max \left\{ 0, \frac{\xi[\Lambda_1 \delta - \mu_1(\theta + \mu_1)]}{\delta(\theta + \mu_1)(\gamma + \mu_2 + \frac{{\sigma_1}^2}{2})} \right\} < 1.$$

It is not difficult to observe that

$$\begin{aligned} \min \left\{ \frac{\alpha \Lambda_2}{\mu_2(\gamma + \mu_2 + \frac{{\sigma_1}^2}{2})}, \frac{\alpha^2}{2{\sigma_2}^2(\gamma + \mu_2 + \frac{{\sigma_1}^2}{2})} \right\} & \leqslant \frac{\alpha \Lambda_2}{\mu_2(\gamma + \mu_2 + \frac{{\sigma_1}^2}{2})}, \\ \max \left\{ 0, \frac{\xi[\Lambda_1 \delta - \mu_1(\theta + \mu_1)]}{\delta(\theta + \mu_1)(\gamma + \mu_2 + \frac{{\sigma_1}^2}{2})} \right\} & \geqslant 0, \end{aligned}$$

and $\sigma_1^2 > \frac{2\alpha\Lambda_2}{\mu_2} - 2\gamma - 2\mu_2$ deduces $\frac{\alpha\Lambda_2}{\mu_2(\gamma+\mu_2+\frac{1}{2}{\sigma_1}^2)} < 1$. Then we obtain

$$\min \left\{ \frac{\alpha \Lambda_2}{\mu_2(\gamma + \mu_2 + \frac{{\sigma_1}^2}{2})}, \frac{\alpha^2}{2{\sigma_2}^2(\gamma + \mu_2 + \frac{{\sigma_1}^2}{2})} \right\} - \max \left\{ 0, \frac{\xi[\Lambda_1 \delta - \mu_1(\theta + \mu_1)]}{\delta(\theta + \mu_1)(\gamma + \mu_2 + \frac{{\sigma_1}^2}{2})} \right\} \leqslant \frac{\alpha \Lambda_2}{\mu_2(\gamma + \mu_2 + \frac{{\sigma_1}^2}{2})} < 1.$$

By theorem 2, $\limsup_{t\to\infty} \frac{1}{t} \log C(t) < 0$ *a.s.*, the proof is complete.

Corollary 2. For the model (1), if the condition ${\sigma_2}^2 > \frac{\alpha^2}{2(\gamma+\mu_2)}$ is satisfied, then for any initial values, it holds that $\limsup_{t\to\infty}\frac{1}{t}\log C(t) < 0$ *a.s.*

Proof. Continuing the analysis of the conditions in Theorem 2, we can see that

$$\min\left\{\frac{\alpha\Lambda_2}{\mu_2(\gamma+\mu_2+\frac{{\sigma_1}^2}{2})}, \frac{\alpha^2}{2{\sigma_2}^2(\gamma+\mu_2+\frac{{\sigma_1}^2}{2})}\right\} \leqslant \frac{\alpha^2}{2{\sigma_2}^2(\gamma+\mu_2)},$$

$$\max\left\{0, \frac{\xi[\Lambda_1\delta-\mu_1(\theta+\mu_1)]}{\delta(\theta+\mu_1)(\gamma+\mu_2+\frac{{\sigma_1}^2}{2})}\right\} \geqslant 0,$$

and ${\sigma_2}^2 > \frac{\alpha^2}{2(\gamma+\mu_2)}$ deduces $\frac{\alpha^2}{2{\sigma_2}^2(\gamma+\mu_2)} < 1$. Then we obtain

$$\min\left\{\frac{\alpha\Lambda_2}{\mu_2(\gamma+\mu_2+\frac{{\sigma_1}^2}{2})}, \frac{\alpha^2}{2{\sigma_2}^2(\gamma+\mu_2+\frac{{\sigma_1}^2}{2})}\right\} - \max\left\{0, \frac{\xi[\Lambda_1\delta-\mu_1(\theta+\mu_1)]}{\delta(\theta+\mu_1)(\gamma+\mu_2+\frac{{\sigma_1}^2}{2})}\right\} \leqslant \frac{\alpha^2}{2{\sigma_2}^2(\gamma+\mu_2)} < 1.$$

By theorem 2, $\limsup_{t\to\infty}\frac{1}{t}\log C(t) < 0$ *a.s.*, the proof is complete.

Corollary 3. For the model (1), if the condition $\Lambda_1\delta > \mu_1(\theta+\mu_1)$ and $\frac{\xi[\Lambda_1\delta-\mu_1(\theta+\mu_1)]}{(\theta+\mu_1)\delta} > \frac{\alpha\Lambda_2}{\mu_2} - \gamma - \mu_2$ are satisfied, then for any initial values, it holds that $\limsup_{t\to\infty}\frac{1}{t}\log C(t) < 0$ *a.s.*

Proof. Using the same method in Corollary 1, we obtain

$$\max\left\{0, \frac{\xi[\Lambda_1\delta-\mu_1(\theta+\mu_1)]}{\delta(\theta+\mu_1)(\gamma+\mu_2+\frac{{\sigma_1}^2}{2})}\right\} = \frac{\xi[\Lambda_1\delta-\mu_1(\theta+\mu_1)]}{\delta(\theta+\mu_1)(\gamma+\mu_2+\frac{{\sigma_1}^2}{2})} > 0,$$

under the condition $\Lambda_1\delta > \mu_1(\theta+\mu_1)$. Moreover,

$$\min\left\{\frac{\alpha\Lambda_2}{\mu_2(\gamma+\mu_2+\frac{{\sigma_1}^2}{2})}, \frac{\alpha^2}{2{\sigma_2}^2(\gamma+\mu_2+\frac{{\sigma_1}^2}{2})}\right\} \geqslant \frac{\alpha\Lambda_2}{\mu_2(\gamma+\mu_2)},$$

which implies

$$\begin{aligned}&\min\left\{\frac{\alpha\Lambda_2}{\mu_2(\gamma+\mu_2+\frac{{\sigma_1}^2}{2})}, \frac{\alpha^2}{2{\sigma_2}^2(\gamma+\mu_2+\frac{{\sigma_1}^2}{2})}\right\} - \max\left\{0, \frac{\xi[\Lambda_1\delta-\mu_1(\theta+\mu_1)]}{\delta(\theta+\mu_1)(\gamma+\mu_2+\frac{{\sigma_1}^2}{2})}\right\}\\ &\leqslant \frac{\alpha\Lambda_2}{\mu_2(\gamma+\mu_2)} - \frac{\xi[\Lambda_1\delta-\mu_1(\theta+\mu_1)]}{\delta(\theta+\mu_1)(\gamma+\mu_2+\frac{{\sigma_1}^2}{2})} \leqslant \left[\frac{\alpha\Lambda_2}{\mu_2(\gamma+\mu_2)} - \frac{\xi[\Lambda_1\delta-\mu_1(\theta+\mu_1)]}{\delta(\theta+\mu_1)(\gamma+\mu_2)}\right].\end{aligned}$$

Note that $\frac{\xi[\Lambda_1\delta-\mu_1(\theta+\mu_1)]}{\delta(\theta+\mu_1)} > \frac{\alpha\Lambda_2}{\mu_2} - \gamma - \mu_2$ deduces that $\frac{\alpha\Lambda_2}{\mu_2(\gamma+\mu_2)} - \frac{\xi[\Lambda_1\delta-\mu_1(\theta+\mu_1)]}{\delta(\theta+\mu_1)(\gamma+\mu_2)} < 1$, then we obtain $\limsup_{t\to\infty}\frac{1}{t}\log C(t) < 0$ *a.s.*, the proof is complete.

Appendix D Numerical simulation

Appendix D.1 A Real Case

Based on the numerical values of the system parameters in Table D1 with respect to the morning rush hour, it is not difficult to calculate that

$$\min\left\{\frac{\alpha\Lambda_2}{\mu_2}, \frac{\alpha^2}{2{\sigma_2}^2}\right\} = \frac{\alpha\Lambda_2}{\mu_2} = 0.33.$$

$$\max\left\{0, \frac{\xi[\Lambda_1\delta-\mu_1(\theta+\mu_1)]}{(\theta+\mu_1)\delta}\right\} + \gamma + \mu_2 + \frac{1}{2}{\sigma_2}^2 = \gamma + \mu_2 = 0.313.$$

By Theorem 2, traffic congestion will propagate Figure D1 also validates this results. This study utilizes traffic data obtained from the "2023 Quarterly Report on Urban Traffic in China" and a real-time traffic query API as an illustrative example. A total of 288 real traffic conditions data points were collected at a sampling rate of every five minutes (The proportion of C data source: https://huiyan.baidu.com/). The model parameters were fitted using the least squares method. Considering the switching nature of congestion scenarios, there are separate infection rates and recovery rates for the morning rush hour and the evening rush hour. We set up two independent datasets: The morning rush hour starts at 6:00, ends at 11:30, with initial values of $(I(t0), S(t0), T(t0), F(t0), C(t0), R(t0)) = (0.98, 0.02, 0, 0.9996, 0.0004, 0)$; The evening rush hour starts at 17:00, ends at 21:30, with initial values of $(I(t1), S(t1), T(t1), F(t1), C(t1), R(t1)) = (0.98, 0.02, 0, 0.998, 0.002, 0)$. We fitted the parameters based on scatter data during the morning and evening rush hour. The estimated values of the parameters are shown in Table D1. As shown in Figure D1, both simulated curves and the scatter data of C on the same plot are presented. The y-axis represents the proportion of C, and the x-axis represents the selected time period.

Table D1 Parameters' Values

Parameters	Values in morning rush hour	Values in evening rush hour
Λ_1	0.005	0.005
Λ_2	0.012	0.006
μ_1	0.005	0.005
μ_2	0.012	0.006
θ	0.01	0.01
α	0.330	0.211
γ	0.301	0.195
δ	0.012	0.012
ξ	0	0

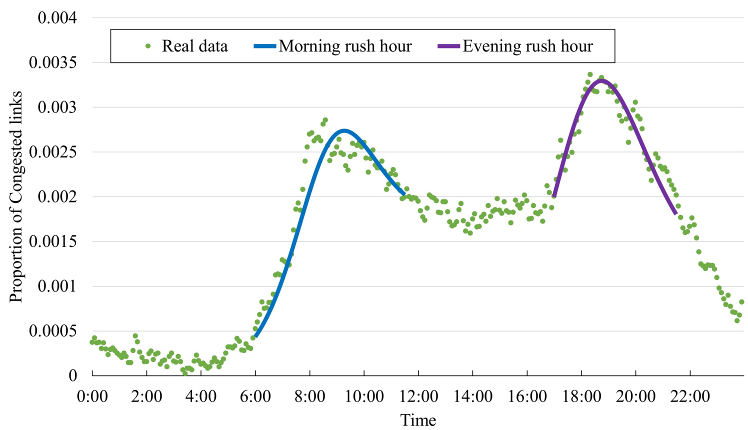

Figure D1 The proportion of congested links $C(t)$ and real scatter data.

Appendix D.2 Control Effect Analysis

Our hybrid control method primarily focuses on effective guidance of congestion information and random clearing strategies. Specifically, the effectiveness of information guidance is determined by the number of participants in information guidance and the intensity of information guidance, corresponding to parameters δ and ξ. The effectiveness of the random clearance strategy corresponds to the guidance intensities σ_1 and σ_2. Therefore, in this section, we compare and analyze the control effects by adjusting the corresponding control intensities δ, ξ, σ_1 and σ_2 based on the aforementioned real case (the evening rush hour in Table D1).

First, we verify the role of information guidance in alleviating traffic congestion. We set the control intensities δ and ξ in the

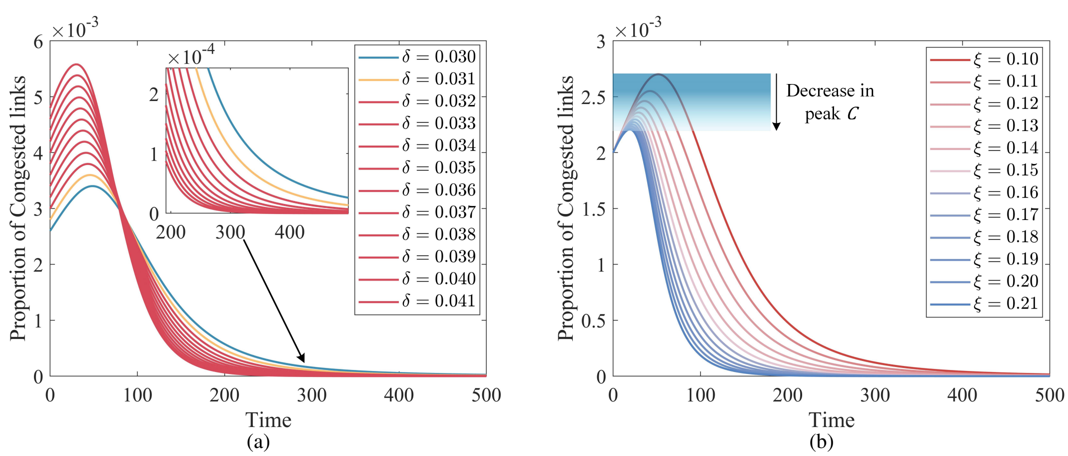

Figure D2 The proportion of congested links $C(t)$: (a) under different parameters $C(0)$ and δ; (b) under different ξ.

Table D2 The proportion of $C(t)$ with the increasing of rate δ from 0.030 to 0.041 with an increment of 0.001 while $\xi = 0.1$.

$\delta(10^{-2})$	3.0	3.1	3.2	3.3	3.4	3.5	3.6	3.7	3.8	3.9	4.0	4.1
Congestion Dissipation Time(min)	455	403	365	337	314	296	281	268	257	247	238	230

Table D3 The proportion of $C(t)$ with the increasing of rate ξ from 0.10 to 0.21 with an increment of 0.01 while $\delta = 0.03$.

$\xi(10^{-2})$	10	11	12	13	14	15	16	17	18	19	20	21
Congestion Dissipation Time(min)	475	420	374	335	302	273	249	227	208	192	178	166
Peak Mitigation Rate(%)	0	5.54	8.84	11.04	12.65	13.91	14.94	15.80	16.55	17.20	17.77	18.28

first row of Table D2 and Table D3. According to Theorem 2, the control intensities met the condition $\xi(\frac{1}{3} - \frac{0.005}{\delta}) > 0.01$, so the congested traffic links will dissipate. As shown in Figure D2, all of the trajectory curves of $C(t)$ eventually tend to zero, and we calculate congestion dissipation time and peak mitigation rate of congestion in the second and third row of Table D2 and Table D3.

Next, we verify the effectiveness of the random controllers through a comparative analysis using experimental data. As shown in Figure D3, this experimental group consists of 6 plots arranged in a 2×3 grid, labeled as Figure D3 (a), (b), (c), (d), (e) and (f), respectively. Figure D3 (a), (b) and (c) represent individual simulation results with three sets of white noise intensities: $\{\sigma_1 = 0, \sigma_2 = 0.2\}$, $\{\sigma_1 = 0, \sigma_2 = 0.4\}$ and $\{\sigma_1 = 0, \sigma_2 = 0.8\}$. Meanwhile, Figure D3 (d), (e) and (f) illustrate the histograms obtained from 10,000 simulations using the parameter values from Figure D3 (a), (b) and (c) to track the numerical value $C(350)$. When $\sigma_1 = 0$ and $\sigma_2 = 0.2$, the condition of Corollary 2 is not met, and therefore, traffic congestion cannot be alleviated. Figure D3 (a) and (d) demonstrate that $C(t)$ still persist. When $\sigma_1 = 0$ and $\sigma_2 \geqslant 0.4$, the condition of Corollary 2 is met, and therefore, traffic congestion can be alleviated. Figure D3 (b), (d) and Figure D3 (c), (f) show that $C(t)$ are effectively suppressed and converge to zero.

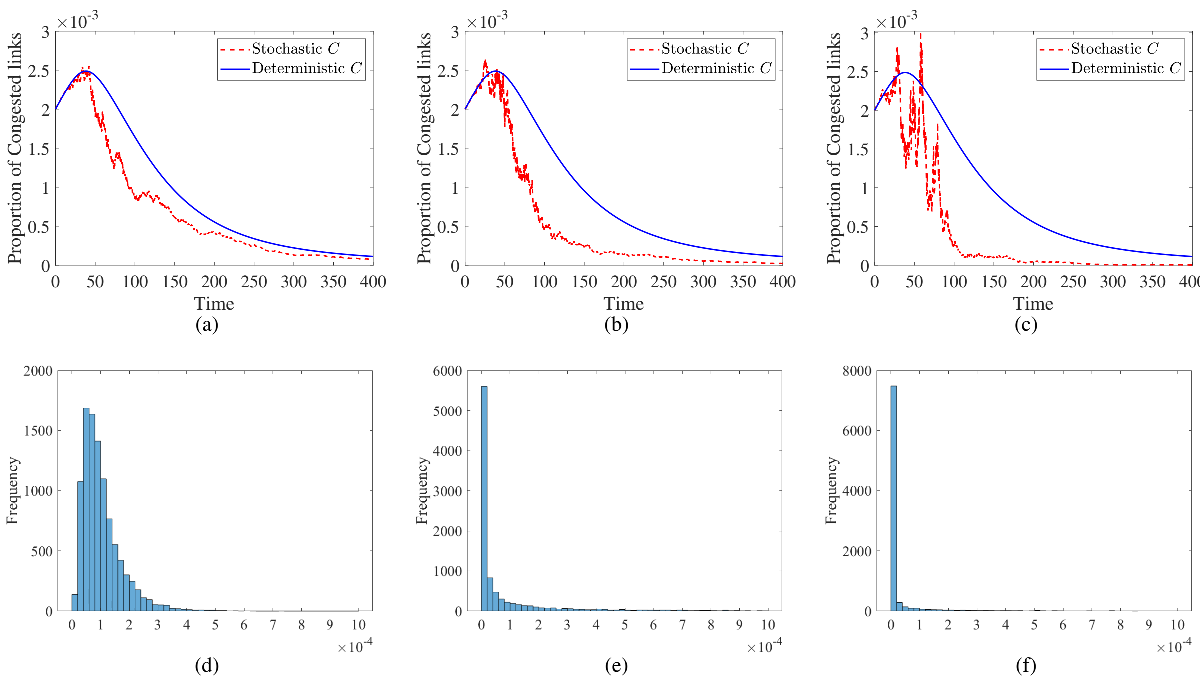

Figure D3 Single random control intensity analysis: (a) and (d) represent state single-sample trajectory plot and statistical graph under $\sigma_2 = 0.2$; (b) and (e) represent state single-sample trajectory plot and statistical graph under $\sigma_2 = 0.4$; (c) and (f) represent state single-sample trajectory plot and statistical graph under $\sigma_2 = 0.8$.

Similarly, as depicted in Figure D4, this experimental group also consists of 6 plots: Figure D4 (a), (b) and (c) represent individual simulation results with three sets of white noise intensities: $\{\sigma_1 = 0.006, \sigma_2 = 0.2\}$, $\{\sigma_1 = 0.024, \sigma_2 = 0.2\}$ and $\{\sigma_1 = 0.096, \sigma_2 = 0.2\}$. Meanwhile, Figure D4 (d), (e) and (f) illustrate the histograms obtained from 10,000 simulations using the parameter values from Figure D4 (a), (b) and (c) to track the numerical value $C(350)$. According to Corollary 1, if $\sigma_2 = 0.2$, $\sigma_1 > 0.02$, traffic congestion can be alleviated. Figure 7 shows that $C(t)$ are effectively suppressed and converge to zero. Moreover, Figure D3 and Figure D4 reveal that as the strength of the two random controllers increases, the proportion of C in the histograms are suppressed to zero, which is consistent with the theoretical analysis in Theorem 2.

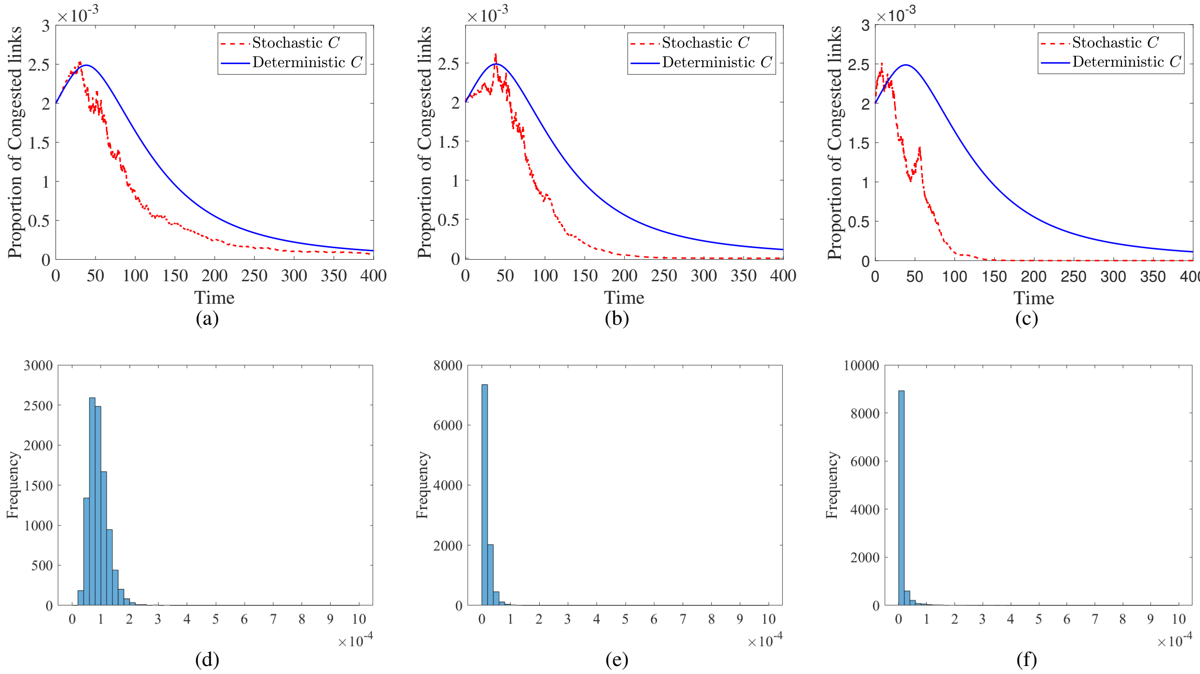

Figure D4 Double random control intensities analysis: (a) and (d) represent state single-sample trajectory plot and statistical graph under $\{\sigma_1 = 0.006, \sigma_2 = 0.2\}$; (b) and (e) represent state single-sample trajectory plot and statistical graph under $\{\sigma_1 = 0.024, \sigma_2 = 0.2\}$; (c) and (f) represent state single-sample trajectory plot and statistical graph under $\{\sigma_1 = 0.096, \sigma_2 = 0.2\}$.

References

1 Mao X, Stochastic differential equations and applications, Elsevier. 2007
2 LaSalle J P. The Stability of Dynamical Systems. Society for Industrial and Applied Mathematics. 1976
3 Yang Q, Mao X. Stochastic dynamical behavior of SIRS epidemic models with random perturbation. Math Biosci Eng, 2014, 11: 1003-1025